Supporting Information for

"A fluorescent molecular rotor showing vapochromism, aggregation-induced emission, and environmental sensing in living cells"

Matthias Koenig,[d] Barbara Storti,[e] Ranieri Bizzarri,[e] Dirk M. Guldi,[d] Giuseppe Brancato*[c] and Giovanni Bottari*[ab]

[a] Departamento de Química Orgánica, Universidad Autónoma de Madrid, 28049, Cantoblanco, Spain

[b] IMDEA-Nanociencia, Campus de Cantoblanco, C/Faraday 9, 28049 Madrid, Spain

[c] Scuola Normale Superiore, Piazza dei Cavalieri 7, I-56126 Pisa, Italy

[d] Department of Chemistry and Pharmacy & Interdisciplinary Center for Molecular Materials (ICMM), Friedrich-Alexander-Universität Erlangen-Nürnberg, 91058, Erlangen, Germany

[e] Materials (ICMM), Friedrich-Alexander-Universität Erlangen-Nürnberg, 91058, Erlangen, Germany

Abbreviations

Cryo−TEM = cryogenic − transmission electron microscopy; DFT = density functional theory; DLS = dynamic light scattering; DMSO = dimethylsulfoxide; **DPAP** = 4-(diphenylamino)-phthalonitrile; n = refractive index of a solvent; NMR = nuclear magnetic resonance; PCM = Polarizable Continuum Model; k_R = radiative decay constant; k_{NR} = non-radiative decay constant; QM = quantum mechanical; TD−DFT = time-dependent density functional theory; TLC = thin layer chromatography; **TPAP** = 4-(triphenylamino)-phthalonitrile; Δf = Lippert-Mataga solvent parameter; ε = dielectric constant; Φ_{fl} = fluorescent quantum yield; τ_R = emission lifetime.

Materials and Methods

Chemicals and solvents were purchased from Aldrich and used without further purification. NMR spectra (^{1}H and ^{13}C) were recorded with a Bruker Advance 300 MHz instrument. IR spectra were recorded on a Bruker Vector 22 spectrophotometer employing in all cases solid samples (KBr pressed disks). EI-MS spectra were obtained from a VG AutoSpec spectrometer. Column chromatography was carried out on silica gel Merck-60 (230-400 mesh, 60Å). Analytical TLC was performed on aluminium sheets precoated with silica gel 60 F-254 from Merck.

Photophysical studies

All solvents were spectroscopic grade and were purchased from various commercial suppliers (Sigma-Aldrich, Merck and Roth). Dielectric constants, refractive indices, and viscosities of the pure solvents were obtained from the literature.[1] UV/vis spectra were recorded with a Perkin Elmer Lambda 2 instrument and steady-state emission with a FluoroMax 3 fluorometer by HORIBA JobinYvon using a quartz cell with 10 mm optical path length. For emission below room temperature, a Haake KT40 thermostat/cryostat was installed, while for emission above room temperature samples were heated using a Haake NB22 thermostat. Fluorescence lifetimes and time-resolved emission were measured with a HORIBA JobinYvon Fluorolog instrument. For excitation, a NanoLED 295 nm and 403 nm light source was used. This instrument was also used to detect emission in the NIR-region. Femtosecond transient absorption studies were performed in argon-saturated solutions with 387 nm excitation laser pulses (1 kHz, 150 fs pulse width) from an amplified Ti:Sapphire laser system (Clark-MXR Inc.) with a laser energy of 200 nJ. Nanosecond laser flash photolysis experiments were carried out with argon or oxygen purged samples using a 355 nm laser pulse from a Quanta-Ray CDR Nd:Yag system (6 ns pulse width) in a front face excitation geometry.

Cryo−TEM studies

For Cryo−TEM studies, a drop of the dispersion (87/13 methanol/water mixture) was put on a lacey carbon-coated copper TEM grid (200 mesh, Science Services) where most of the liquid was removed with blotting paper, leaving a thin film stretched over the grid holes. The specimens were instantly shock vitrified by rapid immersion into liquid ethane and cooled to approximately 90 K by liquid nitrogen in a temperature-controlled freezing unit (Zeiss Cryobox, Zeiss SMT GmbH). The temperature was monitored and kept constant in the chamber during all the sample preparation steps. After the sample is frozen, it was inserted into a cryo-transfer holder (CT3500, Gatan) and transferred to a Zeiss EM922 Omega EF-TEM. Examinations were carried out at temperatures around 90 K at an acceleration voltage of 200 kV. Zero-loss filtered images ($\Delta E = 0$ eV) were taken under reduced dose conditions (100–1000 electrons/nm^2). All images were registered digitally by a bottom-mounted CCD camera system (Ultrascan 1000, Gatan) combined and processed with a digital imaging processing system (Gatan Digital Micrograph 3.9 for GMS 1.82).

DLS studies

DLS data were collected with a Zetasizer Nano ZS in back scatter mode with a He-Ne laser (λ_{exc} = 633 nm) using quartz cells with 10 mm optical path length at 25°C. All measurements were preceded by 1 min. equilibration time and for each probe, 5 measurements consisting of 5 runs each were applied. The DLS measurements imply spherical particles.

Computational details

Quantum mechanical (QM) calculations of the structural and optical properties of **TPAP** have been carried out by methods rooted into density functional theory (DFT) and its time-dependent extension (TD-DFT).[2] Here, a hybrid functional (B3LYP)[3] and its long-range corrected extensions (CAM-B3LYP)[4] has been used, since it was found appropriate for describing molecular systems with an extended electronic delocalization. The 6-31G*(d,p) basis set has been used in all calculations. Solvent effects have been included by means of the conductor-like version of the Polarizable Continuum Model (C-PCM).[5] In particular, an apolar (*i.e.*, hexane) and a polar (*i.e.*, acetonitrile) solvent were considered to investigate polarity effects. Vertical transition energies have been computed within the usual linear response approximation in case of optical absorption, whereas a state-specific PCM calculation has been carried out for optical emission calculations.[6] In the latter case, molecular structures corresponding to the first singlet excited state have been relaxed before emission calculations using analytical gradients.[7] Optical spectra have been evaluated from a convolution of excitation (or emission) calculations on molecular structures generated from a scan about the relevant torsional angle (see Fig. S1). To this end, the 1,2-dicyanobenzene moiety was rotated in step of 10° and the computed excitation (emission) transitions were weighted according to a Boltzmann distribution and, then, Gaussian convoluted (σ = 2000 cm^{-1}). All quantum mechanical calculations have been carried out with the Gaussian09 software package.[8]

Fluorescence microscopy imaging of living cells

Living CHO, placed in glass bottom WillCo dishes, were treated for 15 min with 0.35 ml in 1 ml of a 5.4 mM of **TPAP** solution in DMSO, and then mounted in a thermostated chamber at 37 °C (Leica Microsystems) humidified with 5% CO_2 atmosphere.

Fluorescence imaging was carried out by a confocal scanning laser microscope Leica TCS SP5 (Leica Microsystems, Mannheim, Germany) according to two operating modes: confocal

imaging and confocal FLIM. For confocal imaging, cells were observed by exciting at 405 nm with a pulsed diode laser operating at 40 MHz (average power: 10–20 mW at the sample) and collecting the emission in the 500-580 nm range. Spectral images were collected by acquiring sequentially cell fluorescence in 5-nm emission intervals from 430 to 600 nm. For confocal FLIM, cells were observed by collecting the emission in the 500-580 nm range by a photomultiplier tube interfaced with a Time Correlated Single Photon Counting card and setup (PicoHarp 300, PicoQuant, Berlin); FLIM acquisitions lasted until 100-200 photons were collected on average in each pixel.

In all imaging modes, cells were viewed with a 40 × 1.25 NA or 100 × 1.4 NA oil immersion objectives (Leica Microsystems, Berlin, Germany). Line scanning speeds ranged from 200 to 1400 Hz, depending on the sample fluorescence and optical zoom. The pinhole aperture was set to 1.0 Airy. Imaging data were analyzed by ImageJ software (National Institutes of Health, Bethesda, MD).

For *spectral* phasor analysis, spectral image stacks were elaborated using the Space-Time plugin of ImageJ (available at www.spechron.com/Spectral%20Phasor-Download.aspx).

For *lifetime* phasor analysis, confocal FLIM images were elaborated using SimFCS software (available at www.lfd.uci.edu).

Synthesis of 4-(triphenylamino)-phthalonitrile (TPAP)

TPAP was prepared and purified following a reported procedure.[9] Yield: 88%. ^{1}H NMR (300 MHz, $CDCl_3$) δ (ppm) 8.40 (d, 1H, J = 4.8 Hz); 8.25 (dd, 2H, J = 6.8 Hz); 7.95 (s, 1H); 7.80 (m, 4H), 7.30 (m, 3H), 7.10 (m, 6H); IR (KBr): 3058, 2925, 2855, 2226, 1729, 1583, 1487, 1071, 813; ESI-MS (m/z): $C_{26}H_{17}N_3$ [371.4]: $[M]^+$ 371.4. Elemental analysis for $C_{26}H_{17}N_3$: Calculated: C, 84.07; H, 4.61; N, 11.31; Found C, 84.18; H, 4.68; N, 11.21.

Table S1. This table resumes some physical properties of the solvents, solvent mixtures and PMMA matrix used in this study such as the dielectric constant (ε), the refractive index of the solvent (n) and the Lippert-Mataga solvent parameter (Δf)[10] as well as the fluorescent quantum yield (Φ_{fl}), emission lifetime (τ_R), radiative (k_R) and non-radiative (k_{NR}) decay constant for **TPAP** in the listed solvents. The solvents in the table are organized from the lower (top) to the higher (bottom) Δf values.

Solvent	n	ε	Δf	Φ_{fl}	τ_{fl} (ns)	k_R (ns^{-1})	k_{NR} (ns^{-1})
cyclohexane	1.426	2.023	0	1	2.82	0.3546	0
o-xylene	1.496	2.568	0.0295	0.86	3.55	0.2423	0.0394
anisole	1.518	4.33	0.1122	0.75	4.4	0.1705	0.0568
tetrahydrofurane	1.407	7.52	0.2089	0.47	5.44	0.0864	0.0974
anisole/benzonitrile (6/4)	1.523	12.7	0.2091	0.41	5.67	0.0723	0.1041
dichloromethane	1.424	8.93	0.2172	0.42	6.21	0.0676	0.0934
anisole/benzonitrile (4/6)	1.525	16.9	0.2222	0.37	5.55	0.0667	0.1135
benzonitrile	1.53	25.2	0.2348	0.33	4.68	0.0705	0.1432
n-hexanol	1.418	13.3	0.2430	0.202	3.1	0.0652	0.2574
methyl isopropyl ketone	1.39	12.4	0.2502	0.197	4.55	0.0433	0.1765
dimethylsulfoxide	1.477	48	0.2642	0.034	0.94	0.0362	1.0277
dimethylformamide	1.43	37	0.2754	0.048	1.45	0.0331	0.6566
ethylene glycol	1.432	41.4	0.2761	0.0061	0.14	0.0424	6.9021
acetonitrile	1.344	37.5	0.3055	0.04	1.34	0.0299	0.7164
methanol	1.326	33.8	0.3102	0.0026	0.17	0.0151	5.7988

$$\Delta f = \frac{\varepsilon - 1}{2\varepsilon + 1} - \frac{n^2 - 1}{2n^2 + 1} \quad \text{(eq. S1a)}$$

$$\varepsilon_{MS} = f_A \varepsilon_A + f_B \varepsilon_B$$

$$n_{MS}^2 = f_A n_A^2 + f_B n_B^2 \quad \text{(eq. S1b,c)}$$

In eq. S1a, which allows to calculate the Lippert-Mataga solvent parameter Δf, ε is the dielectric constant and n is the refractive index of the solvent. Eq. 1b,c were used to calculate the dielectric constant and refractive index of the solvent mixtures.

$$k_R = \Phi_{fl}/\tau_R \quad \text{(eq. S2a)}$$

$$k_{NR} = (1 - \Phi_{fl})/\tau_R \quad \text{(eq. S2b)}$$

Eq. S2a allows to calculate the radiative decay rate constants. Eq. 2b was used to calculate the non-radiative decay rate constants.

Table S2. Lippert-Mataga polarity parameter (Δf) and non-radiative decay constants k_1 and k_2 as determined from transient absorption spectroscopy for **TPAP** in solvents with variable polarities and viscosities (at 293-298 K)

Solvent	Δf	η (cP)	k_1 (ns^{-1})	k_2 (ns^{-1})
o-xylene	0.0295	0.81	10.0	0.23
tetrahydrofuran	0.2089	0.48	11.8	0.17
acetonitrile	0.3055	0.34	31	0.88
methanol	0.3102	0.52	90	5.19
ethylene glycol	-	16.9	28	3.6
ethylene glycol/glycerol (1:1)	*nd*	115	15	3.0
glycerol	-	1179	9.4	1.4

Table S3: Emission lifetimes and amplitudes for **TPAP** (4.5×10^{-5} M) in methanol and in 87/13 (v/v) methanol/water dispersions.

	τ_1 (ns)	τ_2 (ns)	A1 (%)	A2 (%)
methanol **TPAP** solution	0.17	–	–	–
TPAP dispersion	12.9	3.9	55	45
frozen **TPAP** dispersion	14.3	4.4	50	50

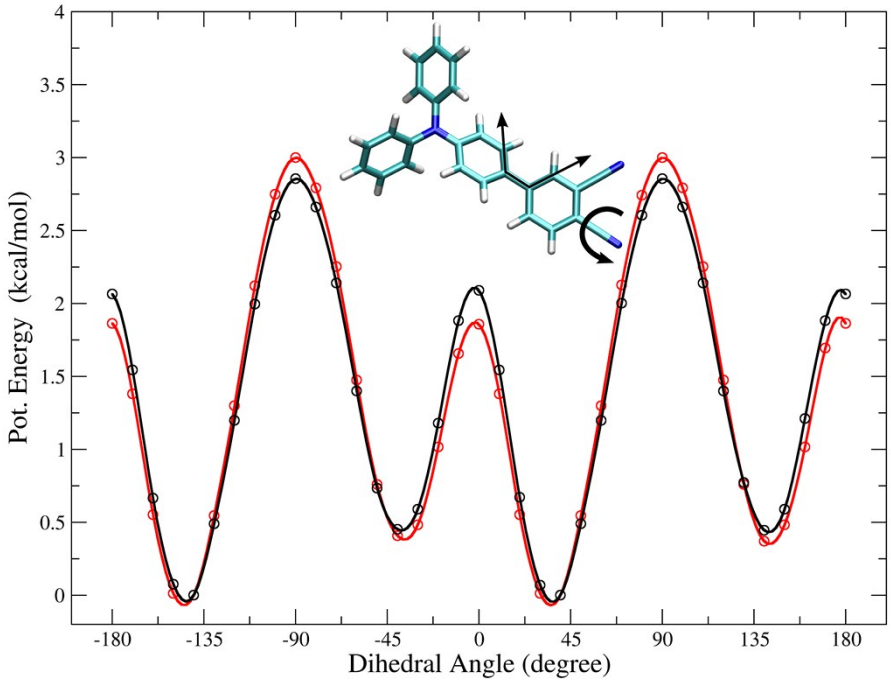

Figure S1: Computed torsional potential of the 1,2-dicyanobenzene moiety with respect to the rest of the molecule in hexane (black) and acetonitrile (red). The considered dihedral angle and rotational motion are depicted along with the molecular structure. QM calculations were performed according to the B3LYP/6-31G*(d,p) level of theory, including solvent effects implicitly.

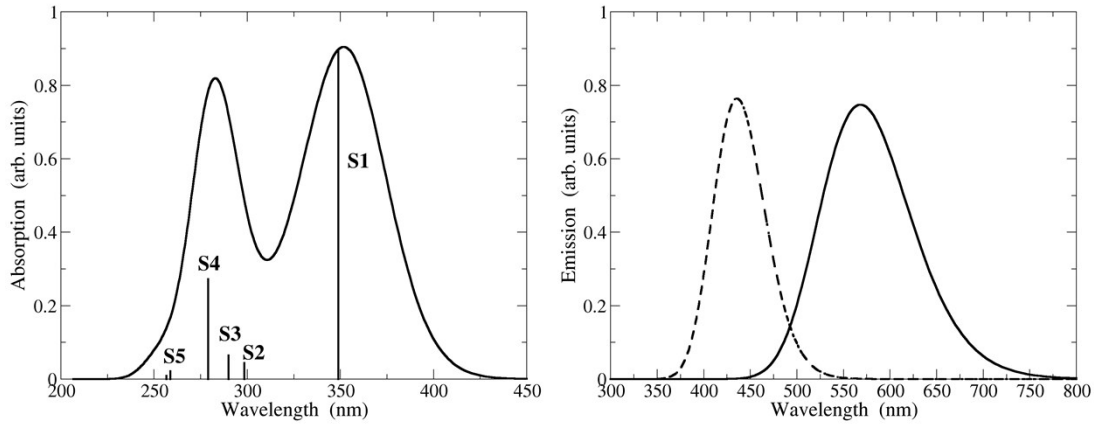

Figure S2: Computed optical absorption (left panel) and emission (right panel) spectra of **TPAP** in solution. Excitation transition energies and intensities are also shown as a stick spectrum in absorption. Solid line, acetonitrile; dashed line, hexane.

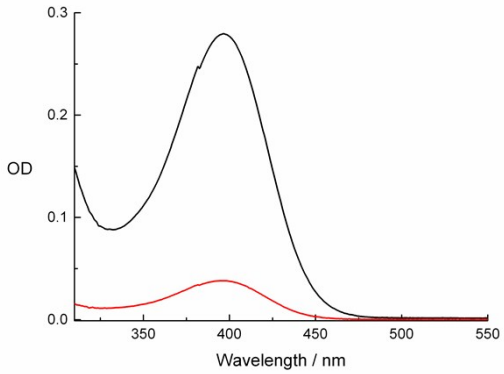

Figure S3: Absorption spectra of **TPAP** (2.5×10^{-6} M) in pyridine (black) and dichloromethane (red).

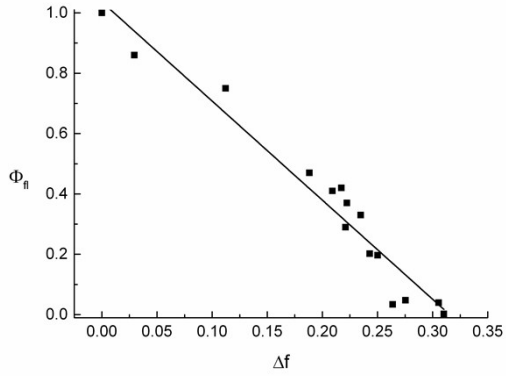

Figure S4: Plot of the Lippert-Mataga solvent parameter (Δf) *vs* the fluorescence quantum yield (Φ_{fl}) of **TPAP** in various solvents.

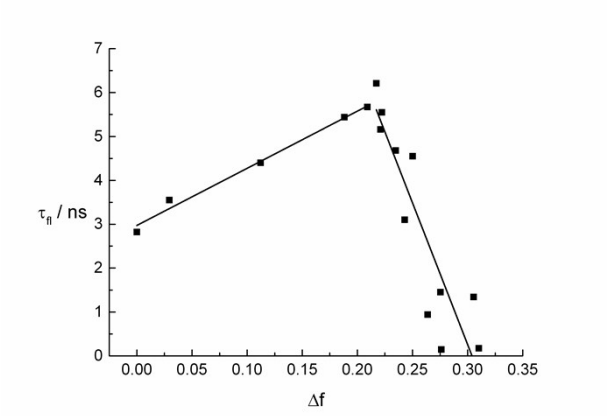

Figure S5: Plot of the fluorescence lifetimes (τ_{fl}) of **TPAP** as a function of the solvent parameter Δf.

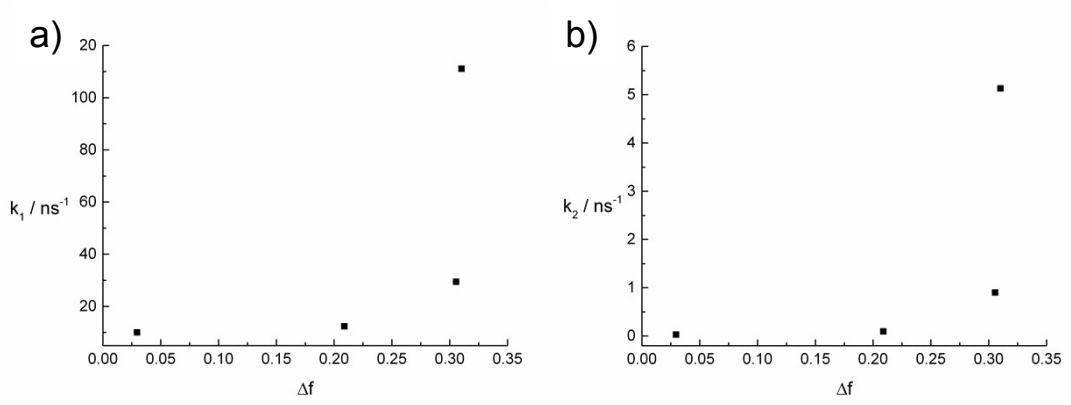

Figure S6: Plot of the Lippert-Mataga solvent parameter (Δf) *vs* a) the decay rate constant k_1 and b) the decay rate constant k_2 for **TPAP** in argon-saturated *o*-xylene, THF, acetonitrile and methanol obtained upon femtosecond flash photolysis.

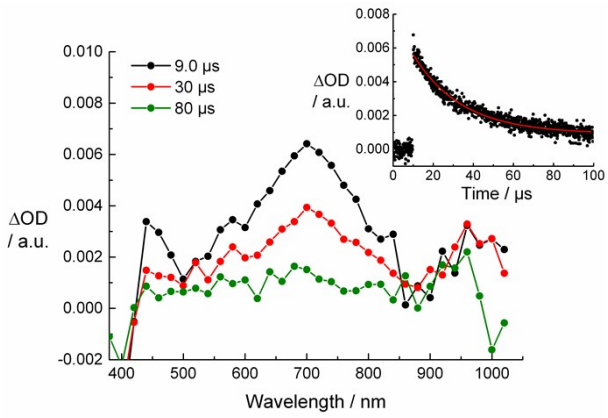

Figure S7: Differential absorption spectra obtained upon nanosecond flash photolysis of **TPAP** in argon-saturated THF with different time delays. OD at the 355 nm excitation wavelength was 0.2. Inset: Corresponding time-absorption profile at 720 nm.

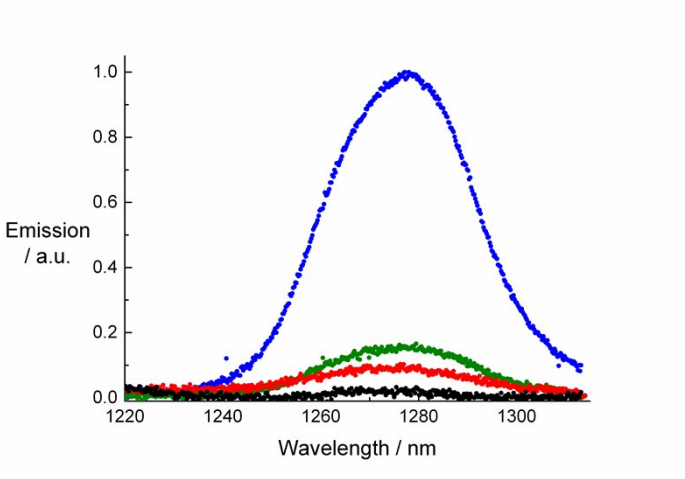

Figure S8: Singlet oxygen phosphorescence spectra of **TPAP** in *o*-xylene (green), THF (red), and acetonitrile (black) as well as the reference free-base tetraphenylporphyrin (blue) measured at room temperature in oxygen saturated solutions. OD at the excitation wavelength (403 nm) was 0.1 for all samples.

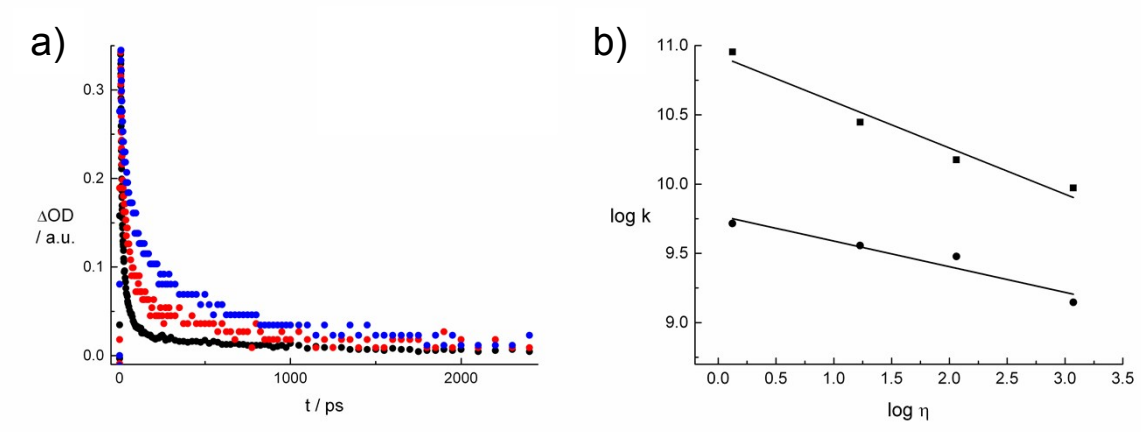

Figure S9: (a) Time–absorption profiles in ethylene glycol (black), ethylene glycol/glycerine (1:1; v/v) (red) and glycerine (blue) at around 900 nm obtained from femtosecond flash photolysis experiments (λ_{exc} = 387 nm). (b) Double-logarithmic plot of the solvent viscosity (η) *vs* the non-radiative decay constants k_1 (squares) and k_2 (circles) as determined from transient absorption spectroscopy for **TPAP** based on the Förster-Hoffmann equation.

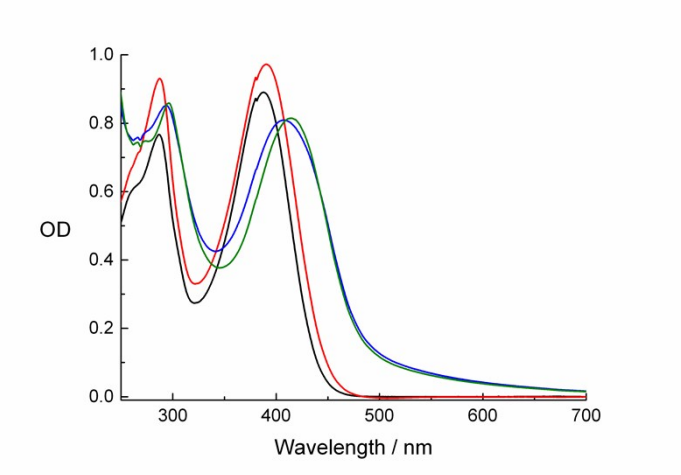

Figure S10: Absorption spectra of **TPAP** (4.5×10^{-5} M) in methanol (black) and in different water/methanol mixtures (45/55 (v/v) (red), 55/34 (v/v) (blue) and 87/13 (v/v) (green)).

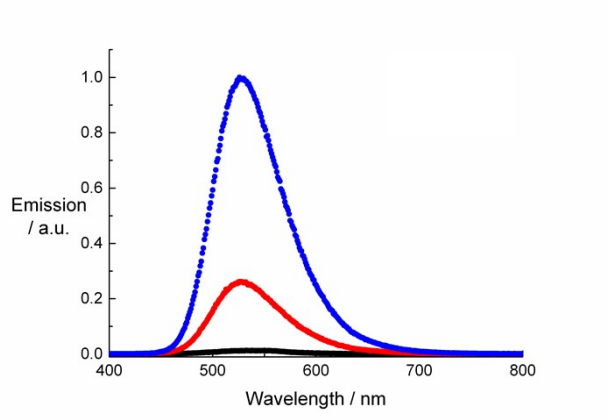

Figure S11: Emission spectra (λ_{exc} = 390 nm) of **TPAP** dispersions (87/13 (v/v) water/methanol mixture) at different concentrations, 1.1×10^{-6} M (black), 2.3×10^{-6} M (red) and 6.8×10^{-6} M (blue).

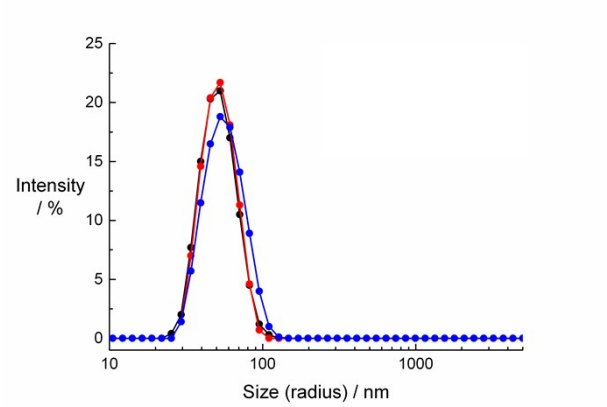

Figure S12: DLS of **TPAP** dispersions at different concentrations ([**TPAP**] = 2.25×10^{-5} M (black), 4.5×10^{-5} M (red), 5.0×10^{-4} M (blue)) in a 87/13 (v/v) water/methanol mixture.

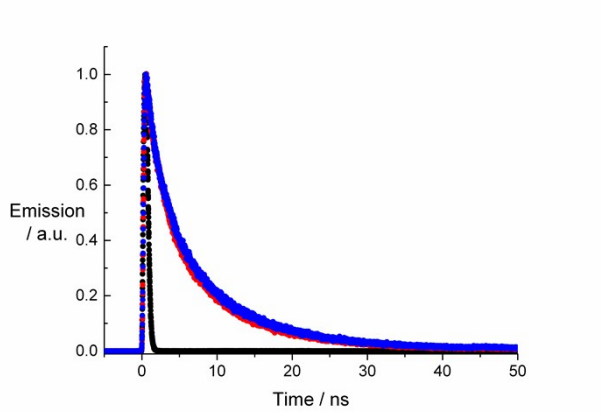

Figure S13: Time fluorescence profiles of **TPAP** (4.5×10^{-5} M) in methanol (black) and in an 87/13 (v/v) water/methanol mixture at room temperature (red) and frozen (blue).

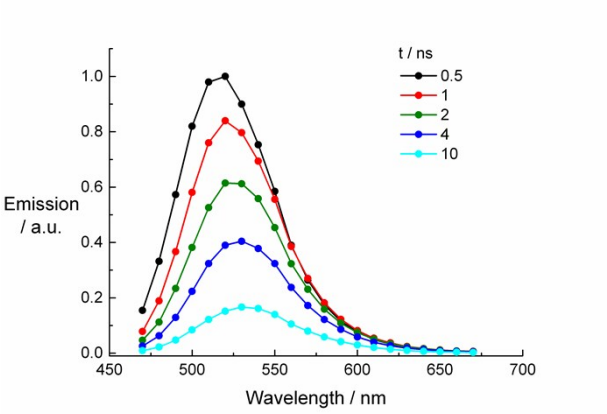

Figure S14: Time-resolved fluorescence spectra of a dispersion of **TPAP** ([**TPAP**] = 4.5×10^{-5} M, 87/13 (v/v) water/methanol mixture) after different time delays.

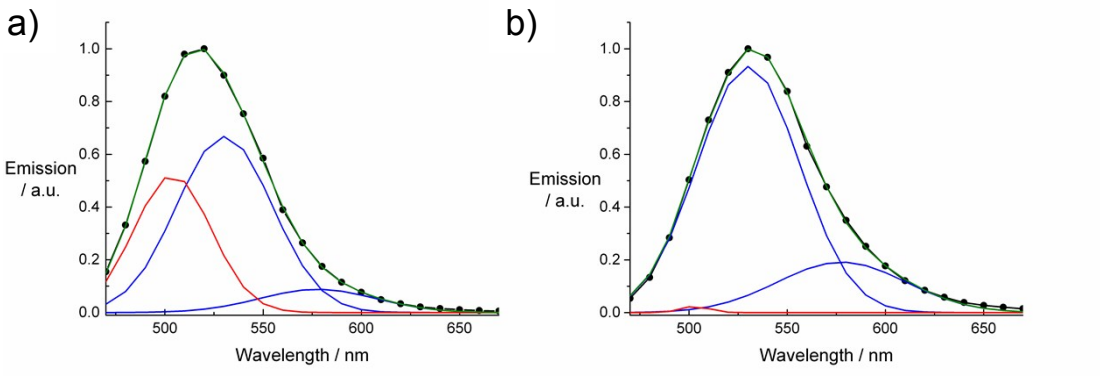

Figure S15: Deconvolution of the time-resolved fluorescence spectra of a dispersion of **TPAP** ([**TPAP**] = 4.5×10^{-5} M, 87/13 (v/v) water/methanol mixture) (black) after a) 0.5 ns and b) 10 ns. The Gauss functions (blue and red) and a sum fit (green) are included.

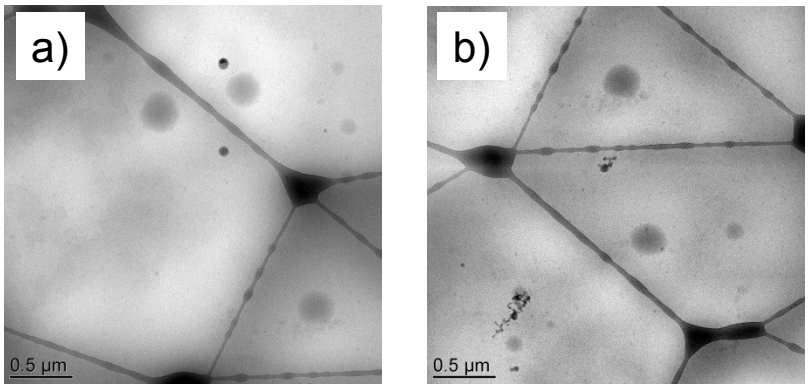

Figure S16: a,b) Cryo-TEM pictures of 87/13 (v/v) water/methanol dispersions of TPAP at 4.5×10^{-5} M.

Supporting references section

1. a) H. G. O. Becker, *Einführung in die Photochemie*, Georg Thieme Verlag, Stuttgart, 1983. b) I. M. Smallwood, *Handbook of Organic Solvent Properties*, Elsevier, 1996. c) M. Holdefer, *Relative Dielektrizitätskonstante εr (DK-Werte) von flüssigen und festen Medien*, Endress+Hauser Messtechnik GmBH+Co., Weil am Rhein, 1999. d) N. P. Cheremisinoff, *Industrial Solvents Handbook*, 2nd edition, Princeton Energies Resources International, Rockville, Maryland, U.S.A., 2003. e) N. S. Cheng, *Ind. Eng. Chem. Res.*, 2008, **47**, 3285–3288.
2. a) E. Runge and E. K. U. Gross, *Phys. Rev. Lett.,* 1984, **52**, 997–1000. b) M. E. Casida, Time-Dependent Density-Functional Response Theory for Molecules, in *Recent Advances in Density Functional Methods Volume 1*, ed. D. P. Chong, World Scientific, Singapore, 1995, pp 155–192.
3. a) A. D. Becke, *J. Chem. Phys.*, 1993, **98**, 5648–5652. b) P. J. Stephens, F. J. Devlin, C. F. Chabalowski and M. J. Frisch, *J. Chem. Phys.*, 1994, **98**, 11623–11627.
4. T. Yanai, D. P. Tew and N. C. A. Handy, *Chem. Phys. Lett.*, 2004, **393**, 51–57.
5. a) A. Klamt and G. Schüürmann, *J. Chem. Soc., Perkin Trans. 2*, 1993*,* 799–805. (b) V. Barone and M. Cossi, *J. Chem. Phys. A*, 1998, **102**, 1995–2001. (c) M. Cossi, N. Rega, G. Scalmani and V. Barone, *J. Comput. Chem.*, 2003, **24**, 669–681.
6. R. Improta, V. Barone, G. Scalmani and M. J. Frisch, *J. Chem. Phys.*, 2006, **125**, 054103.
7. G. Scalmani, M. Frisch, B. Mennucci, J. Tomasi, R. Cammi and V. Barone, *J. Chem. Phys*., 2006, **124**, 094107.
8. M. J. Frisch, G. W. Trucks, H. B. Schlegel, G. E. Scuseria, M. A. Robb, J. R. Cheeseman, G.

Scalmani, et al. “Gaussian 09, Revision B.01,” 2009.

9. L. Giribabu, V. K. Singh, Ch. Vijay Kumar, Y. Soujanya, P. Yella Reddy and M. Lakshmi Kantam, *Sol. Energy*, 2011, **85**, 1204–1212.

10. a) E. Z. Lippert, *Naturforsch.* **1955**, *10a*, 541. b) N. Mataga, Y. Kaifu, M. Koizumi, Bull. Chem. Soc. Jpn., 1956, **29,** 465−470. c) J. R. Lakowicz, *Principles of Fluorescence Spectroscopy*; Plenum Press: New York, 2006.